Electronic Supplementary Information (ESI) for

Multiresponsive chemosensing and photocatalytic properties of three luminescent coordination polymers derived from bifunctional 1,1'-Di(4-carbonylphenyl)-2,2'-biimidazoline ligand

Jun Wang,*[a] Ning-Ning Chen,[a] Jin Qian,[a] Xuan-Rong Chen,[a] Xin-Yue Zhang,[a] and Liming Fan*[b]

[a]*School of Chemistry & Environmental Engineering, Yancheng Teachers University, Yancheng, 224007, China.*
[b]*Department of Chemistry, College of Science, North University of China, Taiyuan 030051, China.*

E-mail: wjyctu@hotmail.com; *limingfan@nuc.edu.cn.*

Table of Contents

Table S1 Crystal data and structure refinement parameters of **1–3**

CP	**1**	**2**	**3**
Formula	$C_{20}H_{24}CdN_4O_{10}$	$C_{63}H_{45}Cd_4Cl_2N_{13}O_{14}$	$C_{20}H_{14}N_4O_5Zn$
Formula weight	592.84	1728.66	455.75
Crystal system	Monoclinic	Hexagonal	Trigonal
Space group	$P2_1/c$	$P6_1$	R-3
a (Å)	12.4871(10)	16.2489(13)	32.2321(19)
b (Å)	14.3971(12)	16.2489(13)	32.2321(19)
c (Å)	16.4209(10)	45.5303(17)	14.2264(11)
α (°)	90	90	90
β (°)	114.354(5)	90	90
γ (°)	90	120	120
V(Å^3)	2689.4(4)	10411(2)	12800(2)
Z	4	6	18
D_{calcd} (Mg/m^3)	1.464	1.637	1.022
μ(mm^{-1})	0.867	1.355	0.887
Temperature (K)	296(2)	291(2)	291(2)
F(000)	1200	5052	3996
R_{int}	0.0208	0.0062	0.0252
R_1 $[I > 2\sigma(I)]^a$	0.0421	0.0317	0.0383
wR_2 $[I > 2\sigma(I)]^b$	0.1283	0.1034	0.0923
Gof	1.075	1.032	1.091

$R_1 = \Sigma| |F_o|-|F_c| |/\Sigma|F_o|$. $\omega R_2 = \Sigma[w(F_o^2-F_c^2)^2]/\Sigma[w(F_o^2)^2]^{1/2}$

Table S2 Selected bond lengths (Å) and angles (º) for **1–3**

CP **1**							
Cd(1)-O(1)	2.450(3)	Cd(1)-O(2)	2.323(3)	Cd(1)-O(5)	2.410(4)	Cd(1)-O(4)#1	2.237(3)
Cd(1)-N(4)#2	2.292(3)	Cd(1)-N(2)#3	2.352(3)				
O(2)-Cd(1)-O(1)	54.49(11)	O(5)-Cd(1)-O(1)	109.88(16)	O(2)-Cd(1)-O(5)	86.46(14)	N(2)#3-Cd(1)-O(1)	86.92(11)
N(4)#2-Cd(1)-O(1)	146.72(11)	O(4)#1-Cd(1)-O(1)	80.06(14)	N(2)#3-Cd(1)-O(5)	161.04(14)	N(4)#2-Cd(1)-O(5)	81.50(14)
O(4)#1-Cd(1)-O(5)	83.25(15)	O(2)-Cd(1)-N(2)#3	111.12(10)	N(4)#2-Cd(1)-N(2)#3	89.12(9)	O(4)#1-Cd(1)-N(2)#3	91.39(13)
N(4)#2-Cd(1)-O(2)	96.90(10)	O(4)#1-Cd(1)-O(2)	126.08(13)	O(4)#1-Cd(1)-N(4)#2	133.09(13)		
Symmetry codes: #1 -x+2,-y,-z+1; #2 -x+1,y-1/2,-z+1/2; #3 x,-y+1/2,z+1/2.							
CP **2**							
Cd(1)-Cl(1)	2.459(2)	Cd(1)-O(5)	2.422(7)	Cd(1)-O(13)	2.262(6)	Cd(1)-O(10)#4	2.263(6)
Cd(1)-N(2)	2.301(6)	Cd(2)-Cl(2)	2.513(3)	Cd(2)-O(6)	2.170(6)	Cd(2)-O(9)	2.265(6)
Cd(2)-O(13)	2.274(6)	Cd(2)-N(3)#5	2.232(7)	Cd(3)-O(7)	2.305(5)	Cd(3)-O(8)	2.402(5)
Cd(3)-O(1)#7	2.302(7)	Cd(3)-O(2)#7	2.375(5)	Cd(3)-N(6)#6	2.230(6)	Cd(3)-N(11)#3	2.264(6)
Cd(4)-N(10)	2.282(7)	Cd(4)-O(3)#6	2.392(5)	Cd(4)-O(4)#6	2.354(6)	Cd(4)-O(11)#9	2.283(5)
Cd(4)-O(12)#9	2.392(5)	Cd(4)-N(7)#8	2.284(6)				
O(10)#4-Cd(1)-O(13)	87.4(2)	O(10)#4-Cd(1)-N(2)	94.6(2)	O(13)-Cd(1)-N(2)	176.2(2)	O(10)#4-Cd(1)-O(5)	81.9(2)
O(13)-Cd(1)-O(5)	82.6(2)	N(2)-Cd(1)-O(5)	94.4(2)	O(10)#4-Cd(1)-Cl(1)	160.62(19)	O(13)-Cd(1)-Cl(1)	80.51(15)
N(2)-Cd(1)-Cl(1)	96.69(17)	O(5)-Cd(1)-Cl(1)	81.59(15)	O(6)-Cd(2)-N(3)#5	104.0(2)	O(6)-Cd(2)-O(9)	97.1(2)
N(3)#5-Cd(2)-O(9)	82.4(2)	O(6)-Cd(2)-O(13)	111.1(2)	N(3)#5-Cd(2)-O(13)	101.9(2)	O(9)-Cd(2)-O(13)	149.2(2)
O(6)-Cd(2)-Cl(2)	90.42(17)	N(3)#5-Cd(2)-Cl(2)	164.27(17)	O(9)-Cd(2)-Cl(2)	89.68(16)	O(13)-Cd(2)-Cl(2)	78.24(16)
N(6)#6-Cd(3)-N(11)#3	106.2(3)	N(6)#6-Cd(3)-O(7)	102.1(2)	N(11)#3-Cd(3)-O(7)	111.2(2)	N(6)#6-Cd(3)-O(1)#7	104.0(3)
N(11)#3-Cd(3)-O(1)#7	83.7(2)	O(7)-Cd(3)-O(1)#7	144.7(2)	N(6)#6-Cd(3)-O(2)#7	85.2(2)	N(11)#3-Cd(3)-O(2)#7	137.9(2)
O(7)-Cd(3)-O(2)#7	105.39(19)	O(1)#7-Cd(3)-O(2)#7	54.2(2)	N(6)#6-Cd(3)-O(8)	158.2(2)	N(11)#3-Cd(3)-O(8)	85.9(2)
O(7)-Cd(3)-O(8)	56.22(16)	O(1)#7-Cd(3)-O(8)	95.1(2)	O(2)#7-Cd(3)-O(8)	97.95(17)	N(7)#8-Cd(4)-N(10)	102.8(2)
N(7)#8-Cd(4)-O(11)#9	108.6(2)	N(10)-Cd(4)-O(11)#9	100.8(2)	N(7)#8-Cd(4)-O(4)#6	83.0(2)	N(10)-Cd(4)-O(4)#6	100.5(2)
O(11)#9-Cd(4)-O(4)#6	152.80(18)	N(7)#8-Cd(4)-O(12)#9	90.89(19)	N(10)-Cd(4)-O(12)#9	155.9(2)	O(11)#9-Cd(4)-O(12)#9	55.64(19)
O(4)#6-Cd(4)-O(12)#9	100.86(18)	N(7)#8-Cd(4)-O(3)#6	138.4(2)	N(10)-Cd(4)-O(3)#6	85.7(2)	O(11)#9-Cd(4)-O(3)#6	109.57(19)
O(4)#6-Cd(4)-O(3)#6	55.50(17)	O(12)#9-Cd(4)-O(3)#6	97.15(18)				
Symmetry codes: #3 y+1,-x+y+1,z-1/6; #4 y,-x+y,z-1/6; #5 x-y,x,z+1/6; #6 x-y+1,x,z+1/6; #7 -y+1,x-y+1,z+1/3; #8 -y+1,x-y,z+1/3; #9 x-y,x-1,z+1/6.							
CP **3**							
O(1)-Zn(1)	1.9031(15)	N(2)-Zn(1)#1	2.0291(18)	N(4)-Zn(1)#2	1.9983(17)	O(3)-Zn(1)#3	1.8885(16)
O(3)#3-Zn(1)-O(1)	117.82(8)	O(3)#3-Zn(1)-N(4)#4	106.07(8)	O(1)-Zn(1)-N(4)#4	117.40(6)	O(3)#3-Zn(1)-N(2)#5	107.80(7)
O(1)-Zn(1)-N(2)#5	101.11(7)	N(4)#4-Zn(1)-N(2)#5	105.50(7)				
Symmetry codes: #1 -x+y-1/3,-x+1/3,z+1/3; #2 x-y+2/3,x+1/3,-z+1/3; #3 -x,-y+1,-z+1; #4 y-1/3,-x+y+1/3,-z+1/3; #5 -y+1/3,x-y+2/3,z-1/3.							

Table S3 Standard deviation and detection limit calculation for Fe^{3+}, $Cr_2O_7^{2-}$ and NZF in **1**

	Fe^{3+}	$Cr_2O_7^{2-}$	NZF
1	597.223388	597.137779	609.978518
2	597.525673	597.251263	609.631232
3	597.021232	597.457365	609.593265
4	597.441231	597.034332	610.012316
5	597.282718	597.001232	609.891231
Standard deviation (σ)	0.17592	0.16547	0.17563
Ksv	1.41×10^4	1.58×10^4	3.78×10^4
Detection limit (3σ/Ksv)	3.74×10^{-5}	3.14×10^{-5}	1.39×10^{-5}

Table S4 Standard deviation and detection limit calculation for Fe^{3+}, $Cr_2O_7^{2-}$ and NZF in **2**

	Fe^{3+}	$Cr_2O_7^{2-}$	NZF
1	502.762131	520.508999	521.254927
2	502.531144	520.421232	521.373216
3	502.827535	520.671313	521.094313
4	502.914577	520.831752	521.512132
5	502.521374	520.412266	521.136545
Standard deviation (σ)	0.15871	0.16094	0.15369
Ksv	1.14×10^4	1.96×10^4	2.87×10^4
Detection limit (3σ/Ksv)	4.18×10^{-5}	2.46×10^{-5}	1.61×10^{-5}

Table S5 Standard deviation and detection limit calculation for Fe^{3+}, $Cr_2O_7^{2-}$ and NZF in **3**

	Fe^{3+}	$Cr_2O_7^{2-}$	NZF
1	439.068312	450.361476	449.693751
2	439.214273	450.413143	449.603243
3	438.912313	450.291399	449.814321
4	439.212645	450.466366	449.513354
5	439.308066	450.781232	449.923171
Standard deviation (σ)	0.13854	0.16942	0.14605
Ksv	1.38×10^{4}	1.35×10^{4}	2.20×10^{4}
Detection limit (3σ/Ksv)	3.01×10^{-5}	3.76×10^{-5}	1.99×10^{-5}

Table S6 Comparison of various CPs sensors for the detection of Fe^{3+}, $Cr_2O_7^{2-}$ and NZF.

	Analyte	CPs-based fluorescent Materials	Quenching constant (K_{SV}, M^{-1})	Detection Limits (DL)	Media	Ref
1	Fe^{3+}	$[H_2N(CH_3)_2]_2[Zn_2L(HPO_3)_2]$	3.96×10^5	1.16×10^{-4} mM	H_2O	21
2		$\{[Tb(Cmdcp)(H_2O)_3]_2(NO_3)_2{\cdot}5H_2O\}_n$	5532	1.5 mM	H_2O	22
3		$\{[Cu^I_2(ttpa)2][Cu^{II}(bptc)]{\cdot}3H_2O{\cdot}DMF\}_n$	3.817×10^3	2.59 μM	H_2O	23
4		$\{[Co_4(timb)_2(Br\text{–}IPA)_4]{\cdot}5H_2O\}_n$	1.79×10^4	3.01×10^{-5} M	H_2O	24
5		$[Tb(HMDIA)(H_2O)_3]{\cdot}H_2O$	1.73×10^4		H_2O	25(a)
6		$\{[Zn(oba)(L)_{0.5}]{\cdot}dma\}_n$	9.3×10^3		DMF/ H_2O	25(b)
		$\{[Cd_2(SA)_2(L)_2]{\cdot}H_2O\}_n$	2.1×10^4	2.4×10^{-6} M	DMF/ H_2O	25(c)
7		$\{[Cd(CDC)(L)]\}_n$	4.9×10^3	7.4×10^{-5} M		
1	$Cr_2O_7^{2-}$	$[Cd_2(L_1)(1{,}4\text{-}NDC)_2]_n$	5.86×10^4	0.031 ppm	H_2O	26
2		$[Zr_6O_4(OH)_8(H_2O)_4(TCPP)_4]$ □9DMF□3.5H_2O	5.91×10^4		H_2O	27
3		$\{[Zn(H_2BCA)(m\text{-}bib)]{\cdot}H_2O\}_n$	5.3×10^4	0.07 μM	H_2O	28
4		$[Zn_5(TDA)_4(TZ)_4]{\cdot}4DMF\}_n$	6.77×10^3		H_2O	29
5		$[Zn(NH_2\text{-}bdc)(4{,}4'\text{-}bpy)]$	7.62×10^3	1.30 μM	H_2O	30
6		$[Cd_{1.5}(L)_2(bpy)(NO_3)]{\cdot}2DMF{\cdot}2H_2O$	5.42×10^4	320 ppb	H_2O	31
1		$\{[Cd_3(TDCPB){\cdot}2DMAc]{\cdot}DMAc{\cdot}4H_2O\}_n$	7.46×10^4		DMAc	32
2		$\{[Tb(TATMA)(H_2O){\cdot}2H_2O\}_n$	3.00×10^4		H_2O	33
3		$[Zn(L)_2]{\cdot}CH_2Cl_2{\cdot}CH_3OH$	1.62×10^4		CH_3OH	34
4		$[Cd(tptc)_{0.5}(o\text{-}bimb)]_n$	4.4×10^4		DMF	35
5		$[Cd(H_2tptc)_{0.5}(mbimb)(Cl)]_n$	2.1×10^5		DMF	
6		$[Zn_2(azdc)_2(dpta)]{\cdot}(DMF)_4$	1.30×10^5	0.63 ppm	DMF	36

$H_3CmdcpBr$ = N-carboxymethyl-(3,5-dicarboxyl)pyridinium bromide;

ttpa = tris(4-(1,2,4-triazol-1-yl)phenyl)amine, H_4bptc = 3,3′,4,4′-biphenyltetracarboxylic acid;

timb=1,3,5-tris(2-methylimidazol-1-yl)benzene;

H_4MDIA= 5,5′-methylenediisophthalic acid;

L = 3,3′-azodipyridine, H_2oba = 4,4′-oxydibenzoic acid;

H_2SA = succinic acid, H_2CDC = 1,4-Cyclohexanedicarboxylic acid, L = [3,3'-azobis(pyridine)];

L1 = 1,4-bis(benzimidazol-1-yl)-2-butylene, 1,4-H_2NDC = 1,4-naphthalenedicarboxylic acid;

H_4TCPP=2,3,5,6-tetrakis(4-carboxyphenyl)pyrazine;

H_2BCA= bis(4-carboxybenzyl)amine, m-bib = 1,3-bis(1-imidazoly)benzene;

H_2TDA = thiophene-2,5-dicarboxylic acid, HTZ = 1H-1,2,4-Triazole;

NH_2-H_2bdc = 2-amino-1,4-benzenedicarboxylic acid, 4,4'-bpy = 4,4'-bipyridine;

HL = 4-(4-carboxyphenyl)-1,2,4-triazole, bpy = 4,4′-bipyridine;

H_6TDCPB = 1,3,5-tris[3,5-bis(3-carboxylphenyl-1-yl)phenyl-1-yl]benzene;

H_3TATMA = 4, 4′,4″-s-triazine-1,3,5-triyltri-m-aminobenzoate

HL = 2-hydroxy-4-(pyridin-4-yl)benzaldehyde

H_4tptc = p-terphenyl-2,2″,5″,5″-tetracarboxylate acid

bimb = ortho/meta-bis(imidazol-1-ylmethyl)benzene

H_2azdc = Azobenzene-4,4'-dicarboxylic Acid

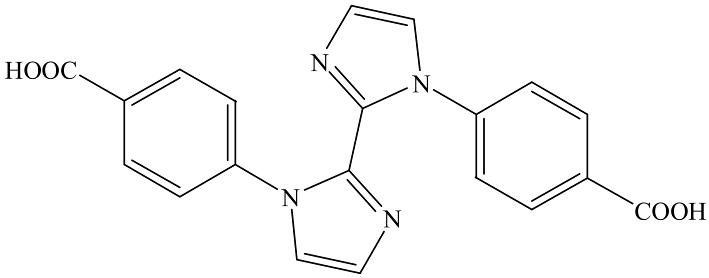

Scheme S1. The structure of 1,1'-di(4-carbonylphenyl)-2,2'-biimidazoline (H_2L)

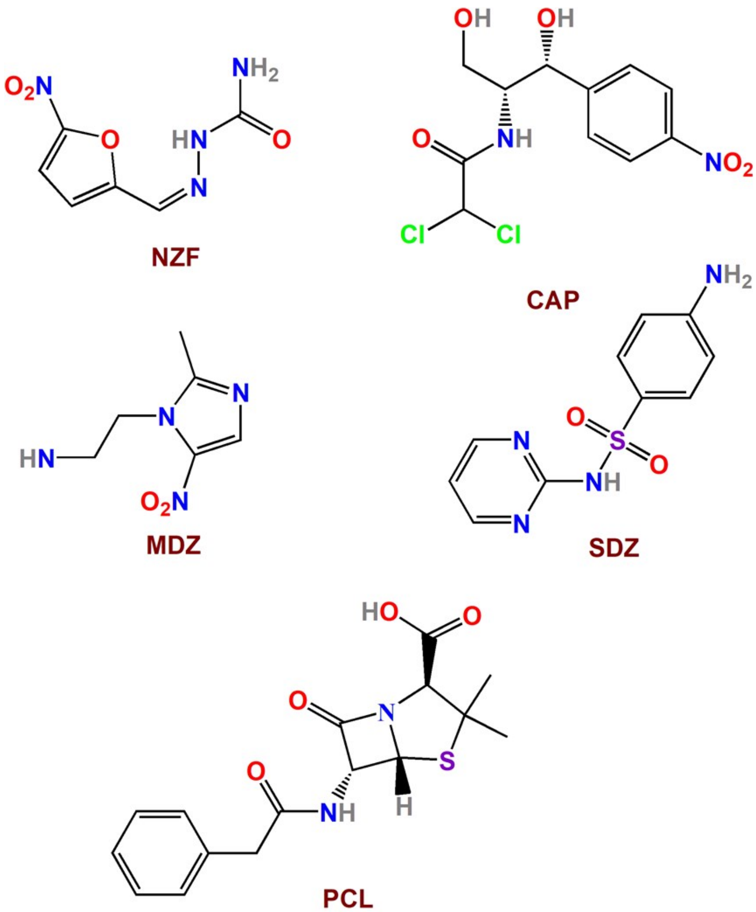

Scheme S2. The structures of selected antibiotics

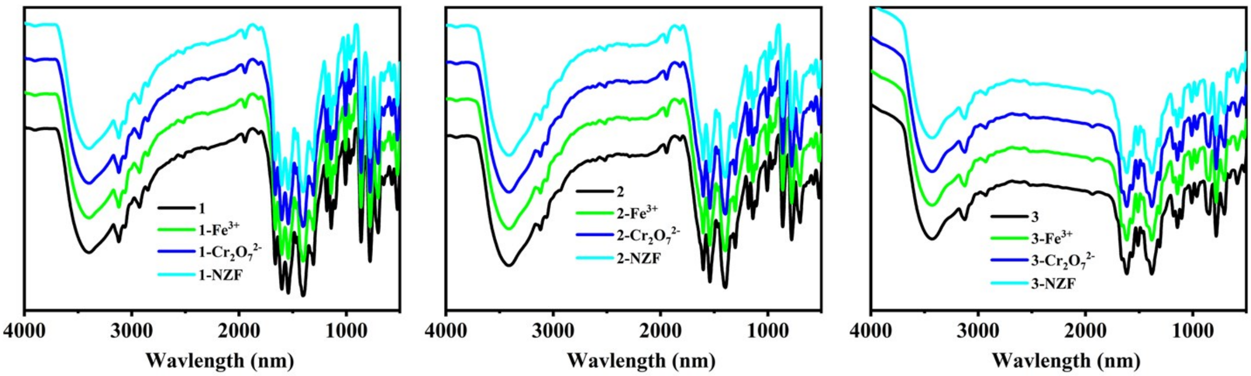

Fig. S1 FT-IR spectra of **1-3** and **1-3** recovered from Fe^{3+}, $Cr_2O_7^{2-}$ and NZF

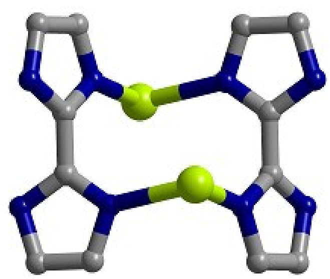

Fig. S2 The binuclear $[Cd_2(BIM)_2]$ SBU in **1**

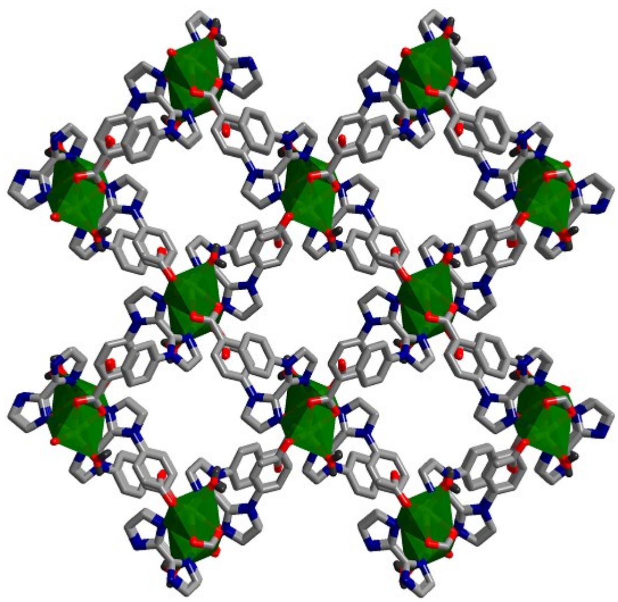

Fig. S3 The 3D porous network with the 1D circular channels of **1**

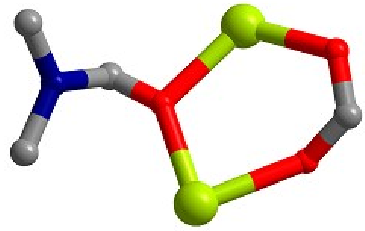

Fig. S4 The binuclear [$Cd_2(COO)_2(DMF)$] cluster in **2**

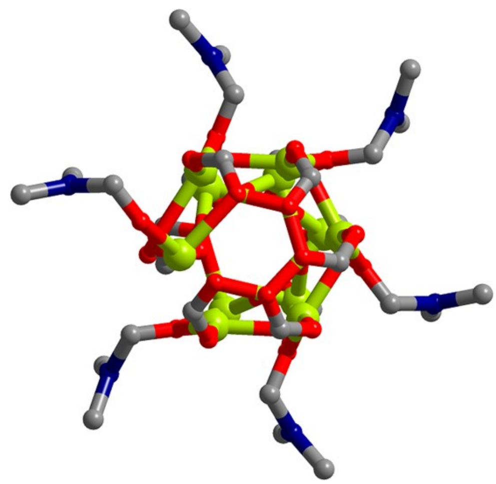

Fig. S5 The 1D [$Cd_2(COO)_2(DMF)$]$_n$ chain with 6-fold helix in **2**

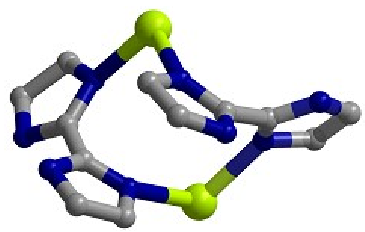

Fig. S6 The binuclear [$Cd_2(BIM)_2$] SBU in **2**

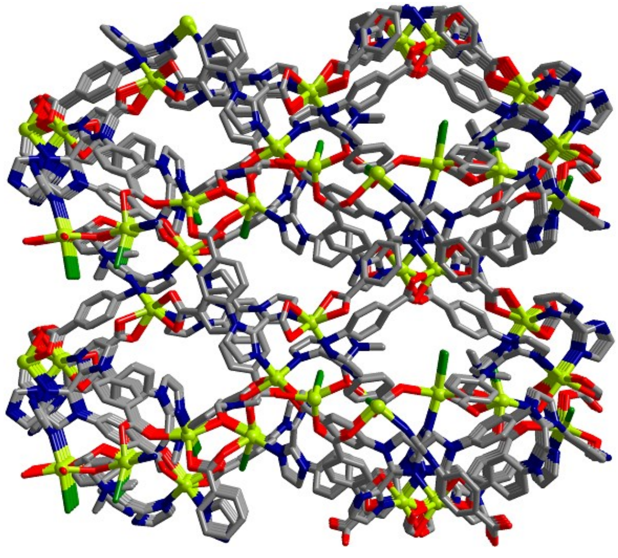

Fig. S7 The 3D porous network of **2**

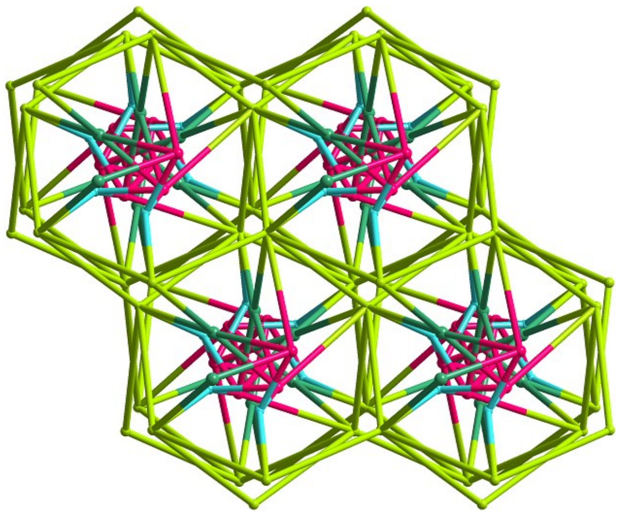

Fig. S8 The 3D 4-nodal (3,4,5,8)-c $\{4.5^2\}\{4^3.5^3\}\{4^3.5^7\}\{4^5.5^{11}.6^7.7^4.8\}$ net of **2**

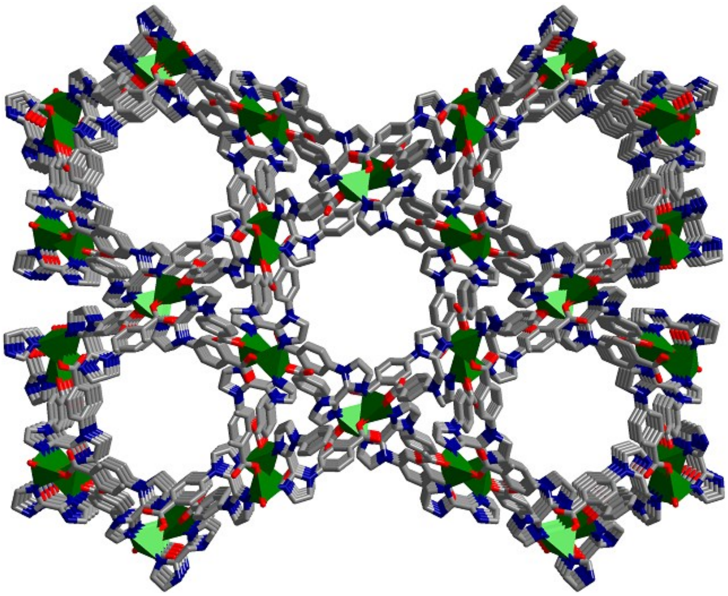

Fig. S9 The 3D porous framework containing the 1D circle channels of **3**

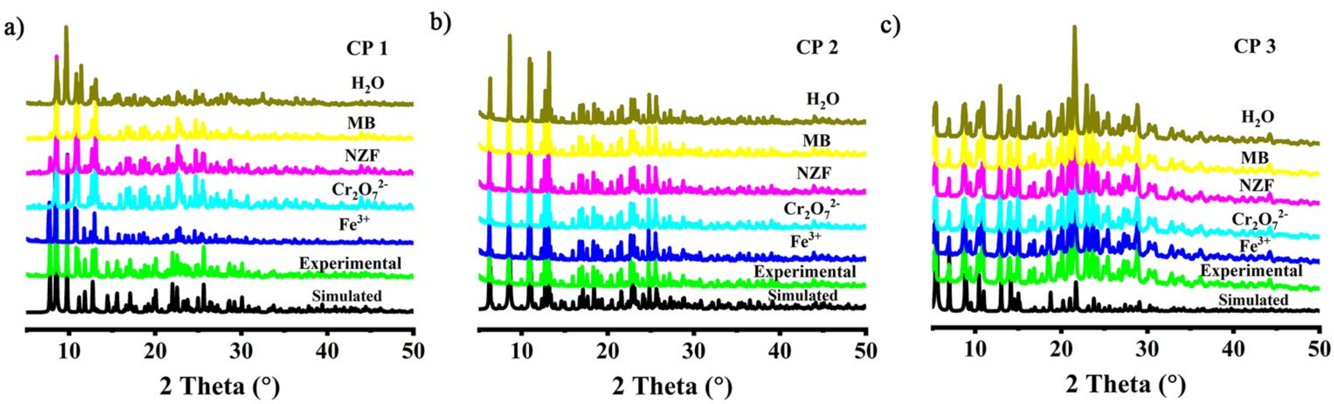

Fig. S10 PXRD patterns of **1-3**

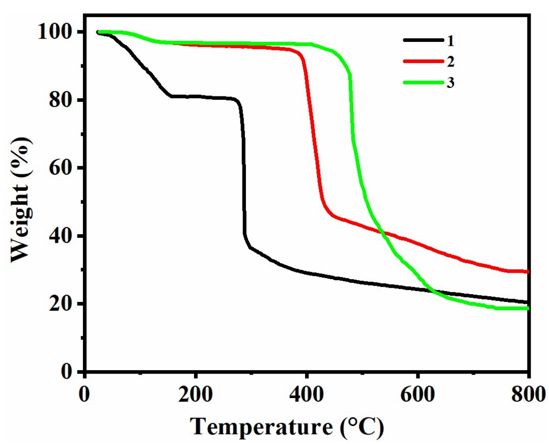

Fig. S11 TGA curves for **1−3**

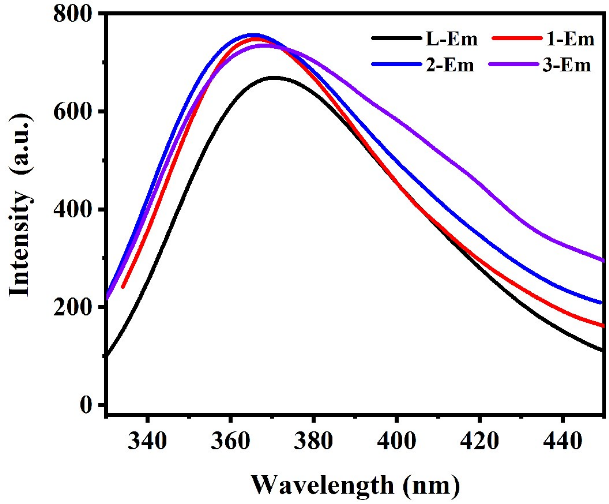

Fig. S12 The solid state diffuse-reflectance spectra for **1**, **2**, **3** and H_2L ligand

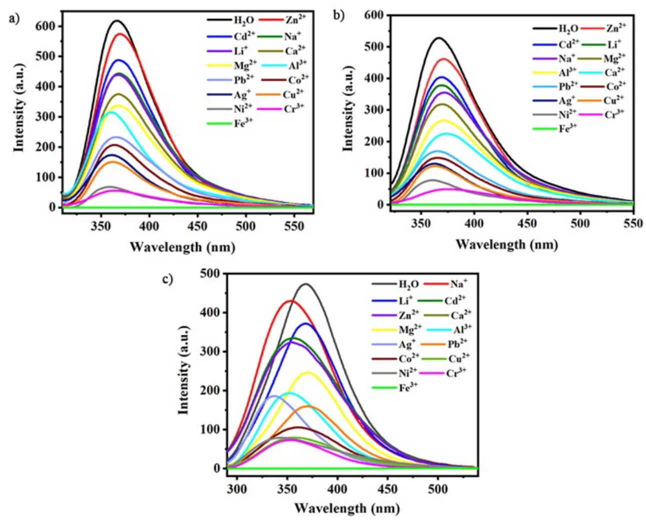

Fig. S13 Fluorescence response of **1**(a), **2**(b) and **3**(c) toward different metal cations in H_2O solution

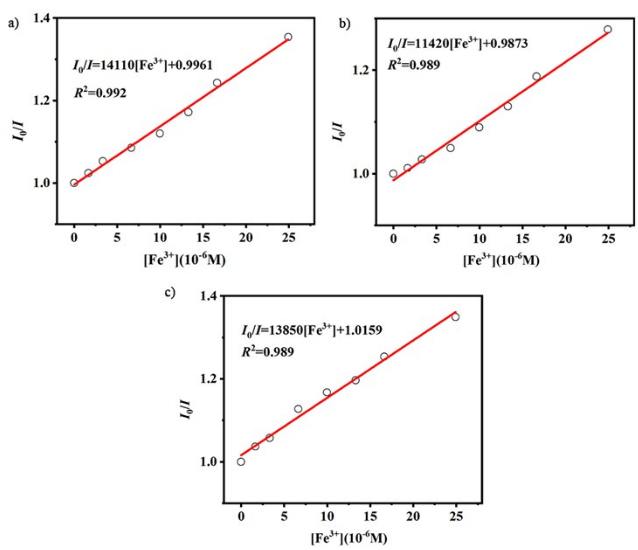

Fig. S14 The stern−Volmer plots of Fe^{3+} in **1**(a), **2**(b) and **3**(c).

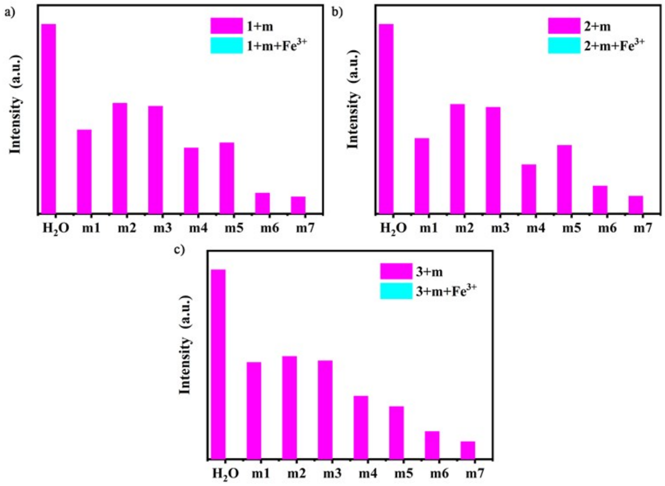

Fig. S15 Luminescence intensity of **1**(a), **2**(b) and **3**(c) with different cations solution added Fe^{3+} ions (10^{-2} M) (m1: Ag^{+}/Na^{+}/Co^{2+}; m2: Li^{+}/Ni^{2+}/Zn^{2+}; m3: Mg^{2+}/Pb^{2+}/Cd^{2+}; m4: Cr^{3+}/Ca^{2+}; m5: Al^{3+}/Cu^{2+}; m6: Ni^{2+}; m7: Cr^{3+}).

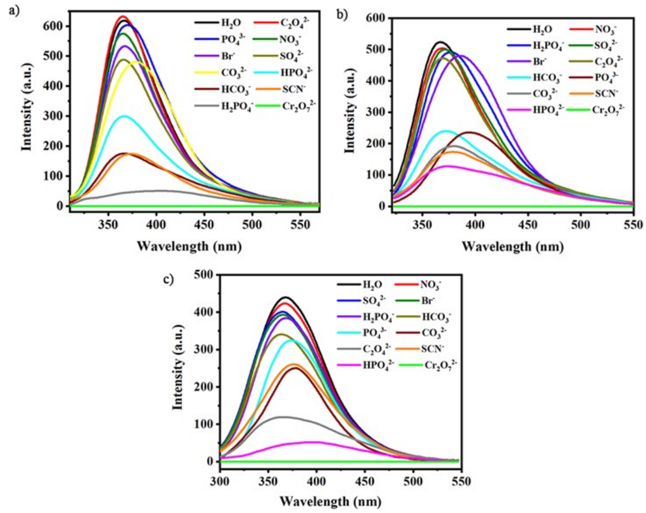

Fig. S16 Fluorescence response of **1**(a), **2**(b) and **3**(c) toward different anions in H_2O solution.

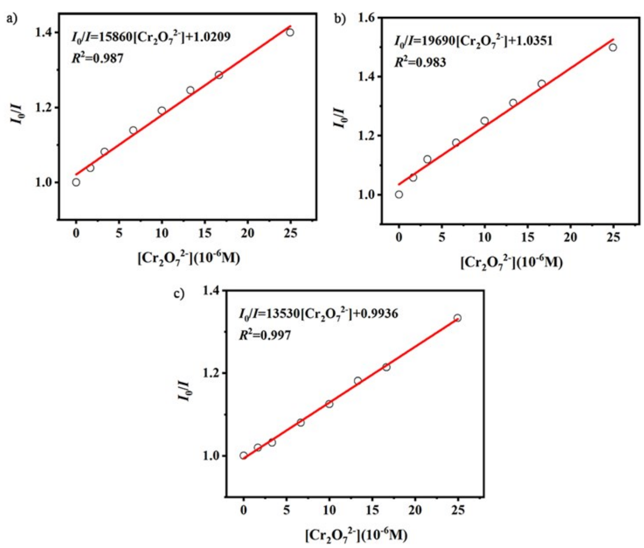

Fig. S17 The stern−Volmer plots of $Cr_2O_7^{2-}$ in **1**(a), **2**(b) and **3**(c).

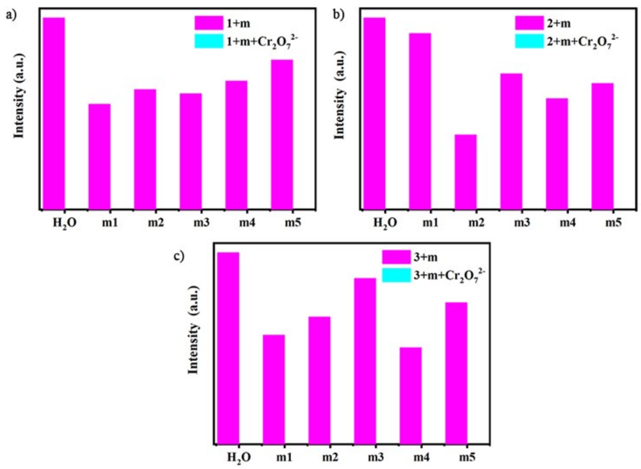

Fig. S18 Luminescence intensity of **1**(a), **2**(b) and **3**(c) with different mixed cations solution added $Cr_2O_7^{2-}$ ions (10^{-2} M) (m1: $C_2O_4^{2-}/H_2PO_4^-$; m2: PO_4^{3-}/SCN^-; m3: NO_3^-/ HCO_3^-; m4: Br^-/HPO_4^{2-}; m5: SO_4^{2-}/ CO_3^{2-}).

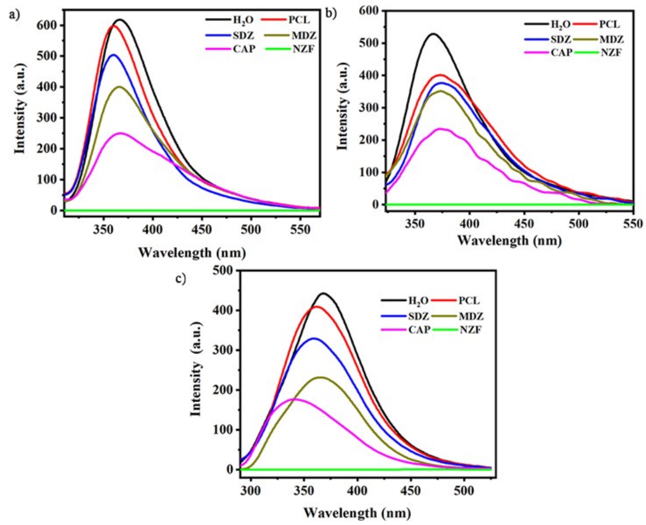

Fig. S19 Fluorescence response of **1**(a), **2**(b) and **3**(c) toward different antibiotics in H_2O solution.

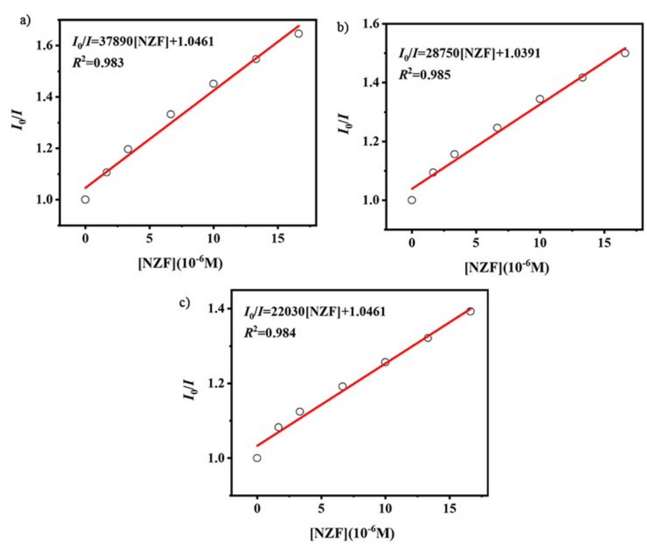

Fig. S20 The stern−Volmer plots of NZF in **1**(a), **2**(b) and **3**(c).

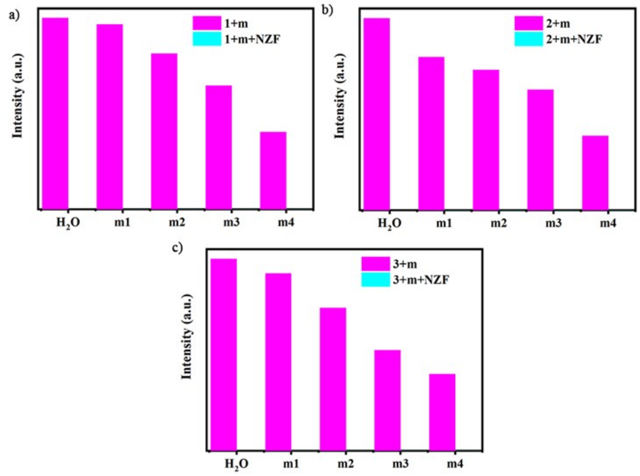

Fig. S21 Luminescence intensity of **1**(a), **2**(b) and **3**(c) with different mixed cations solution added NZF (10^{-2} M) (m1: PCL; m2: SDZ; m3: MDZ; m4: CAP).

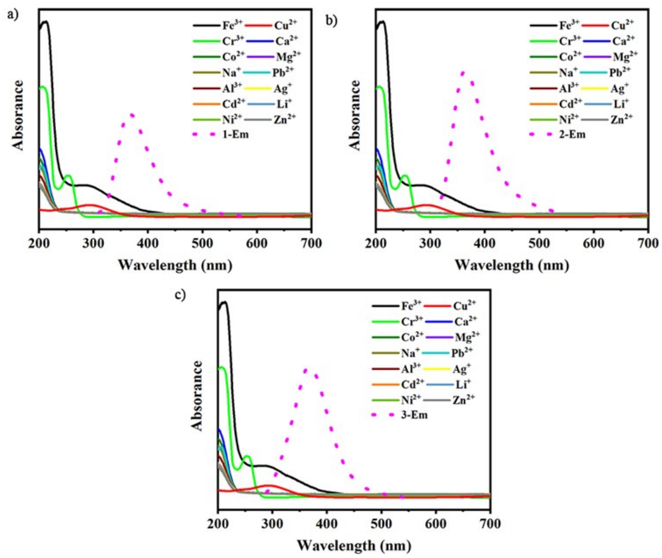

Fig. S22 UV-vis spectra of different cations in H_2O solutions, and the emission spectra of **1**(a), **2**(b) and **3**(c).

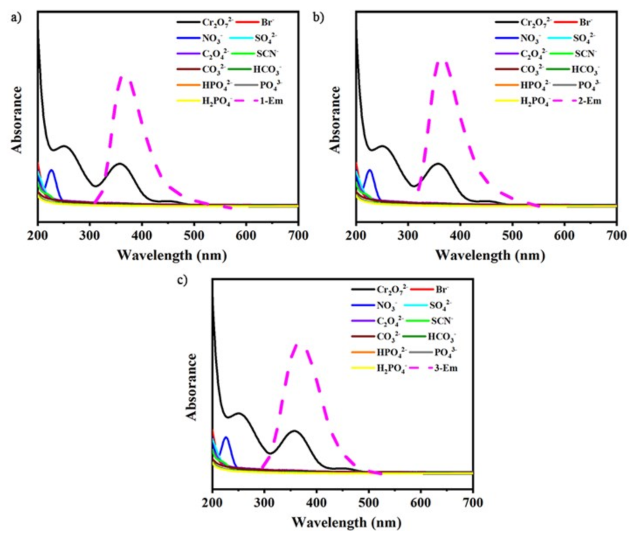

Fig. S23 UV-vis spectra of different anions in H_2O solutions, and the emission spectra of **1**(a), **2**(b) and **3**(c).

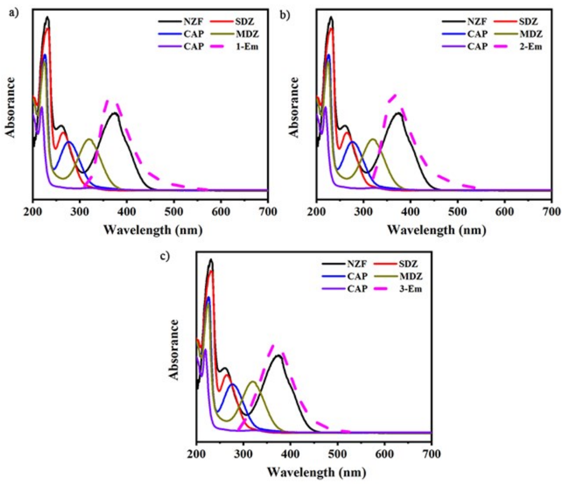

Fig. S24 UV-vis spectra of different antibiotics in H_2O solutions, and the emission spectra of **1**(a), **2**(b) and **3**(c).

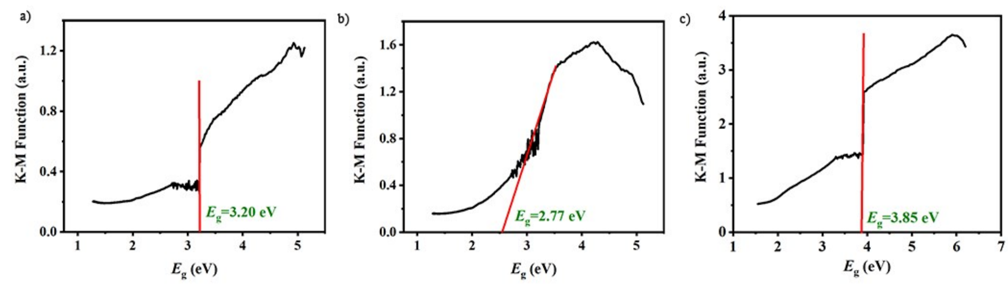

Fig. S25 Kubelka–Munk-transformed diffuse reflectance spectra of **1**(a), **2**(b) and **3**(c).